Automated Vehicle Extraction and Speed Determination From QuickBird Satellite Images

Wen Liu, *Student Member, IEEE*, Fumio Yamazaki, *Member, IEEE*, and Tuong Thuy Vu, *Member, IEEE*

***Abstract*—A new method has been developed to automatically extract moving vehicles and subsequently determine their speeds from a pair of QuickBird (QB) panchromatic (PAN) and multispectral (MS) images. Since the PAN and MS sensors of QB have a slight time lag (approximately 0.2 s), the speed of a moving vehicle can be determined from the difference in the positions of the vehicle observed in the PAN and MS images due to the time lag. An object-based approach can be used to extract a vehicle from the PAN image, which has a resolution of 0.6 m. However, it is difficult to accurately extract the position of a vehicle from an MS image because its resolution is 2.4 m. Thus, an area correlation method is proposed to determine the location of a vehicle from an MS image at a sub-pixel level. The speed of the moving vehicle can then be calculated by using the vehicle extraction results. This approach was tested on several parts of a QB image covering central Tokyo, Japan, and the accuracy of the results is demonstrated in this study.**

***Index Terms*—Correlation, object detection, vehicles, velocity measurement.**

I. Introduction

As THE populations of cities continue to increase, road traffic is reaching levels of congestion that are greater than were anticipated during the planning of these cities and their infrastructure. Introducing vehicle monitoring is an important first step toward solving this problem. Normally, field-based equipment such as cameras installed at fixed locations [1] or radar sensors [2], [3] are used to monitor road traffic. A remote sensing technique has recently emerged as an alternate option to collect traffic information. Using this method, a wider range of information can be collected over a long period of time. Thus, vehicle detection by remote sensing can be extensively used to manage traffic and estimate automobile emissions. It can also provide important information for transportation infrastructure planning.

It is known that the two sensors of some high-resolution satellites, such as Ikonos and QuickBird (QB), have a slight time lag in the acquisition of images (less than 1 s), depending on the scanning mode of the instrument. For example, there is a time lag of approximately 0.2 s between the panchromatic (PAN) image and corresponding multispectral (MS) image acquired by the QB satellite. If a target vehicle that is being observed by the satellite is in motion, the PAN and MS images will record two different positions at different times for the vehicle. The speed and direction of a moving object can be calculated using this position difference [4], [5].

To measure the difference in a vehicle's position from remote sensing images, the images need to be first processed for vehicle extraction. There have been several studies on vehicle detection using remote sensing data. These studies can be categorized into two groups: model-based extraction and data-based extraction. Model-based extraction is based on vehicle models built from a learning process. These models are used to identify whether or not the target is a vehicle. For example, Gerhardinger *et al.* [6] tested an automated vehicle extraction approach based on an inductive learning technique, which was implemented using Features Analyst, an add-in extension of the ArcGIS software. Zhao and Nevatia [7] created a Bayesian network consisting of the features of a vehicle for learning, prior to vehicle detection. Jin *et al.* [8] used a morphological shared-weight neural network to learn an implicit vehicle model and classify pixels into vehicles and non-vehicles. Leitloff *et al.* [9] used a vehicle queue model to extract vehicle queues from a high resolution satellite image and separated the queues into single vehicles.

In data-based extraction, the processing follows a bottom-up procedure to group pixels into objects. Vehicle objects are then discriminated from other objects. Li [10] used a segmentation algorithm based on a fuzzy c-partition to segment color unmanned aerial vehicle (UAV) imagery. Sharma *et al.* [11] investigated three methods for separating vehicles from road pavement from 1-m resolution satellite and airborne imagery. The outlines of vehicles were then extracted by binary mathematical morphology operators. The key to the former approach is a detailed description, which requires a large number of models to cover all types of vehicles. This takes time and cannot be widely applied. The latter approach is simpler and more convenient for widespread use. There were also several studies to extract vehicles from aerial thermal images [12], [13]. These recent studies mainly reported on determining the positions of vehicles with only a few of them [14] considering speed determination or the creation of a traffic information database.

In this study, a new method is developed to automatically extract moving vehicles and subsequently determine their speeds from a QB PAN and MS bundle product. Vehicles can be extracted from a high-resolution (0.6 m) PAN image using an object-based method. Since the resolution of a QB MS image (2.4 m) is not sufficiently high to extract vehicles directly, an

Manuscript received November 15, 2009; revised April 27, 2010 and July 05, 2010; accepted July 20, 2010.

W. Liu and F. Yamazaki are with the Department of Urban Environment Systems, Chiba University, Chiba 265-8522, Japan (e-mail: wen_liu@graduate.chiba-u.jp; yamazaki@tu.chiba-u.jp).

T. T. Vu is currently with the Royal Institute of Technology, Stockholm, Sweden (e-mail: thuy.vu@abe.kth.se).

Color versions of one or more of the figures in this paper are available online at http://ieeexplore.ieee.org.

Digital Object Identifier 10.1109/JSTARS.2010.2069555

Fig. 1. Pan-sharpened QuickBird image of Ninoy Aquino International Airport in Metro Manila, Philippines, from Google Earth. A ghost is observed in front of the airplane that is landing.

area correlation approach is introduced to search for the best-match position by using the result of vehicle extraction from the PAN image. The proposed approach is tested on actual QB and simulated QB images. It is confirmed that the speed of a moving vehicle can be determined by using the vehicle extraction results.

II. Images of Moving Objects in Google Earth

Google Earth (http://earth.google.com/) has recently started providing high-resolution optical images of urban areas. These images consist of either aerial photographs or pan-sharpened QB images. For one scene, a pan-sharpened image can be produced by co-registering a panchromatic (PAN) image and a multispectral (MS) image. However, due to the slight time lag (approximately 0.2 s) seen in a pair of PAN and MS images, the locations of moving objects are displaced. Even if the PAN and MS bands are co-registered for still objects like roads and buildings, they cannot be co-registered for moving objects. This phenomenon was also stated in several papers [14]–[17].

Fig. 1 shows part of Ninoy Aquino International Airport in Metro Manila, Philippines, as seen on Google Earth. Two airplanes can be seen on the runway. The plane on the right is just landing, while the one on the left is standing still and waiting for take-off. A "ghost" can be seen in front of the moving airplane (on the right), and not for the one standing still (on the left). Similar ghosts were observed in images for several other airports around the world, such as Narita/Tokyo International (Japan), Bangkok International (Thailand), and Hong Kong International. These ghosts were produced by the time lag between the PAN and MS sensors of QB. Assuming a time lag of 0.2 s, the speed of the airplane in Fig. 1 can be evaluated as 326 km/h.

Although these kinds of ghosts are also seen in front of other moving objects, like trains, automobiles, and ships, the image resolution limitation and short time lag prevent these ghosts from being as clear as the airplanes. We simulated a higher resolution pan-sharpened image of an expressway with a 0.25 m resolution from an aerial photograph. At this resolution, the ghosts resulting from the time lag between the PAN and MS sensors were clearly seen in front of moving vehicles.

III. Methodology of Object-Based Vehicle Extraction

Since the speed of a moving vehicle is calculated by the location changes seen in a pair of PAN and MS images, the vehicle locations first need to be extracted from the PAN and MS images. Vehicles can be extracted directly from a PAN image with a 0.6 m resolution. In this paper, an object-based method is proposed to extract vehicles from PAN images.

Since vehicles are moving along a road, road extraction should be the first processing step. The focus of the study is on the extraction of vehicles and the determination of their speeds, and hence, a new road extraction approach is not proposed in this paper. There have been numerous studies on road extraction from remote sensing images [18]–[20]. These can easily be employed to extract road objects. However, to avoid the errors that might be included in such automatic road extraction, which would influence the final vehicle extraction results, the roads were extracted manually, with other areas masked off as background.

The pixels in an image are scanned and grouped into objects according to the gray value criteria. In this step, an image represents four kinds of objects: background, roads, vehicles (including their shadows), and other objects treated as noise. The background can be easily discriminated because it has the lowest gray value and a large size. Meanwhile, road surfaces normally show another specific range of gray values. Objects are detected on the basis of two gray value ranges. There might be vehicles that appear to be very similar to the background. Fortunately, the background and roads are often large objects compared with the other objects in an image. These two kinds of objects can be easily extracted on the basis of size thresholds. The remaining pixels are then reformed into objects again on the basis of a local gray value threshold. All the pixels belonging to a car should have similar gray values. Vehicles and their associated shadows generally have a specific range of sizes. This is the criterion used to distinguish them from other objects. Consequently, an initial extraction result is obtained. The flowchart of the proposed approach is shown in Fig. 2.

Commission errors often exist in the initial result; that is, objects other than vehicles are identified as vehicles. Thus, a morphological filter can be added as an option. A verification step is used to separate vehicles and shadows, and to link a vehicle with its associated shadow. Since shadows show very low gray values, they can be discriminated from vehicle objects. Labels are assigned to all of the objects for their identifications (IDs), with shadows and vehicles labeled as -1 and 1, respectively. Subsequently, the associated shadow of a vehicle is sought in its neighborhood. If there is a shadow near a vehicle, it is considered to be cast by this vehicle. Then the vehicle and its associated shadow are reassigned to the same ID. It should be noted that a dark vehicle is often treated as a shadow. As the result, a shadow ID is assigned to it. However, since it has no link with a vehicle, such a dark object is reassigned as a vehicle. Finally, a vehicle database and shadow database are developed. Attributes include the ID, coordinates of the center point, size, and four corner coordinates of a vehicle.

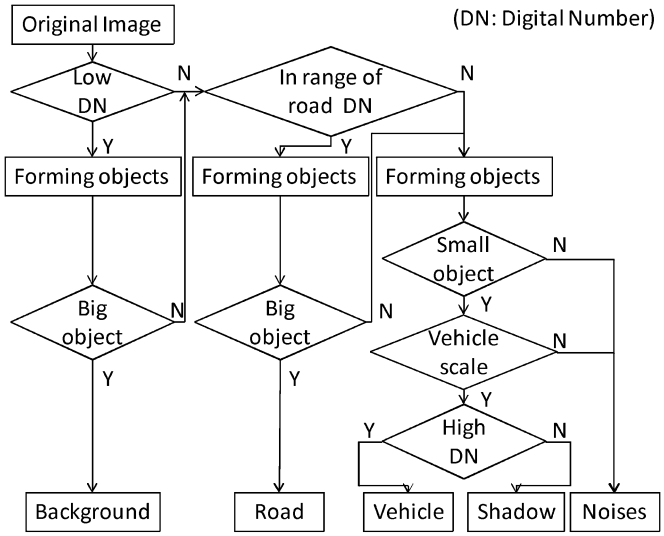

Fig. 2. Flowchart of the proposed object-based vehicle extraction approach.

IV. Vehicle Extraction From a PAN Image

The study area was located in the central part of Tokyo, Japan. Three parts (Study Areas I, II, III) of a QB image that was taken on March 20, 2007 were used in this study. The targets were moving vehicles on urban expressways.

The object-based method was used to extract the vehicles in the three parts of the QB 0.6 m resolution PAN image. First, cubic convolution was used to transform the PAN image into a 0.24 m/pixel image. The roads were extracted manually to avoid the errors involved in automatic road extraction. An area morphological filter [21] was used to remove other irrelevant information such as lines on the road surface. The pixel size was 0.24 m, and the window size of the filter was tested for three cases: 3×3, 5×5, and 7×7 pixels. In case of 3×3 pixels window, some road lines could not be removed by the area morphological filter. In case of 7×7 pixels window, some small vehicles were removed by the filter. The best result was found with a window size of 5×5 pixels; noises were filtered and vehicle shapes were retained completely. In this segmentation process, all of the pixels were scanned and grouped into objects based on the gray value criteria. If the neighbor pixels had the similar value, then they were grouped into an object. Two threshold values were defined from the histogram of the image to estimate roads and background. Several size thresholds were defined to find vehicles from objects. As a result, light colored vehicles are shown in white and shadows or dark vehicles are shown gray in Fig. 3. Additionally, vehicle position and size information was stored in a database for the vehicle extraction from an MS image and the subsequent speed determination.

The vehicle extraction results are compared with visual inspection results in Table I. There were 159 vehicles in the PAN image, and 149 vehicles were extracted correctly by the object-based vehicle extraction. Only 10 vehicles were missed, with 18 noisy areas incorrectly extracted as vehicles. The producer's accuracy was 94%, and the user's accuracy was 89%.

Almost all of the vehicles could be extracted from the PAN image. The object-based method could extract not only light-colored vehicles but also dark-colored ones and some in shadow.

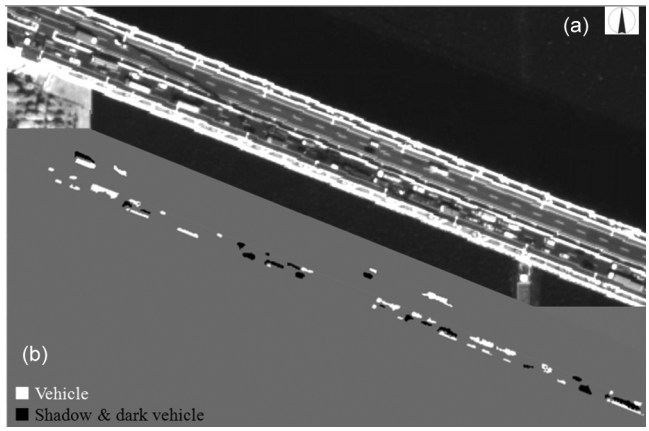

Fig. 3. (a) Original PAN image and (b) results of vehicle extraction from Study Area I of QuikBird.

TABLE I
Accuracy of Object-Based Vehicle Extraction From QuickBird PAN Image

	Vehicle extracted	True counts	correct	Omission	Commission
Scene 1	94	96	92	4	2
Scene 2	9	7	7	0	2
Scene 3	64	56	50	6	14
Total	167	159	149	10	18
	Producer accuracy (correct/true)		User accuracy (correct/extracted)		
	94%		89%		

A few commission errors (wrong extractions) still occurred due to a signboard, its shadow, and some lines on the road.

V. The Methodology of Area Correlation

The object-based approach can be used to extract vehicles from a 0.6 m resolution PAN image. However, the resolution of a corresponding MS image is approximately 2.4 m. Hence, a vehicle appears in only 1 or 2 pixels. Most vehicle pixels are mixed with those of the road, making it difficult to accurately extract the edge and position of a vehicle. The object-based approach cannot extract vehicles from MS images. To determine the speed of a vehicle, the shift in the vehicle's location in a pair of PAN and MS images is required. Thus, an area correlation method is introduced to estimate the location of a vehicle from an MS image at a sub-pixel level.

Area correlation is a method for designating Ground Control Points (GCPs) in image-to-image registration [22]. A small window of pixels (template) from the image to be registered is statistically compared with a region of the reference image, which is bigger than the template image. From the distorted images, templates "T" of M rows by N columns are selected. A bigger size window "S" is selected for the reference image. A template is overlaid on the reference image and a similarity index is calculated. This procedure is carried out for every possible position in the reference image, and a similarity matrix is obtained. This similarity matrix contains the values of the statistical comparison between the template and the reference image. The position in the similarity matrix, where the similarity index

reaches a maximum value, represents the necessary offset that the template has to move horizontally and vertically to match the reference image.

One of the similarity indexes is the cross-correlation coefficient between the template and the reference image (1). The cross-correlation coefficient, r_{ij}, is a scalar quantity in the interval $[-1.0, 1.0]$. The cross-correlation coefficient can be used as a similarity index since it gives a measure of the degree of correspondence between the reference and template, or can be seen as a coefficient describing how well two sample populations vary jointly [23].

$$r_{ij}=\frac{\sum_{m=1}^{N}\sum_{n=1}^{N}(T_{m,n}-\mu_T)(S_{i+m,j+n}-\mu_S)}{\left[\sum_{m=1}^{N}\sum_{n=1}^{N}(T_{m,n}-\mu_T)\right]^{1/2}\left[\sum_{m=1}^{N}\sum_{n=1}^{N}(S_{i+m,j+n}-\mu_S)\right]^{1/2}} \quad (1)$$

where μ_T and μ_S represent the average values for the template and the search image, respectively, and i and j show the location of the template in the search image.

The database obtained after the object-based vehicle extraction from a PAN image is used to extract vehicles from an MS image. Using the location information of a vehicle in the database, the vehicle and the surrounding road are selected as a template. A reference image is selected that has the same center point as the template but is larger in the direction of movement. The cross-correlation coefficient between the two areas is calculated by sliding the template over the reference image and multiplying the two arrays pixel by pixel. The maximum correlation point indicates the vehicle position in the MS image with the highest probability. The template and reference images are first transformed into 0.24 m/pixel images by cubic convolution. Then, the template and reference images can be matched at a sub-pixel level, at 1/10 the pixel size of the MS image.

VI. Vehicle Extraction From MS Images

The three parts of the QB MS image and the results of the vehicle extraction from the corresponding PAN image were used to test the area correlation method. Since an MS image has four multispectral bands (Blue, Green, Red, and Near-Infrared), it needed to be transformed into a one-band image before the area correlation analysis. Principal Component Analysis (PCA) was employed to transform the MS image into a new 4-band image. The first component image with the highest variance (more than 80%) was used to calculate the cross-correlation coefficient with the corresponding PAN image. To match the template and reference images at a sub-pixel level, both the PAN and MS images were transformed into 0.24 m/pixel images by cubic convolution.

Using the vehicle location information, the template was made 5 pixels larger in each direction than the vehicle object extracted from the PAN image. Then, a reference image was selected from the MS image around the location of the template. The maximum moving speed was set as 120 km/h considering the speed limit of the urban expressway, and thus the maximum movement in the time lag between the PAN and MS images was approximately 7 m, which was 29 pixels in the 0.24 m/pixel image. A reference image was selected that was 29 pixels bigger than the template image in the direction of motion. Since the road and vehicle pixels were mixed together in the MS image, the reference image was also made 5 pixels larger than the template in the other directions to improve the accuracy of the area correlation method; e.g., if a vehicle object occupied 25×17 pixels in an image, and a 35×27 pixel template image was selected from the resized PAN image (0.24 m/pixel), a 69×37 pixel reference image was selected from the resized MS image (0.24 m/pixel). The cross-correlation coefficient of each shift was calculated as a matrix, as shown in Fig. 4. The location of the maximum correlation was the upper-left point of the template in the reference image. All of the vehicle templates in the PAN image and their detected locations from the MS image are shown in Fig. 5.

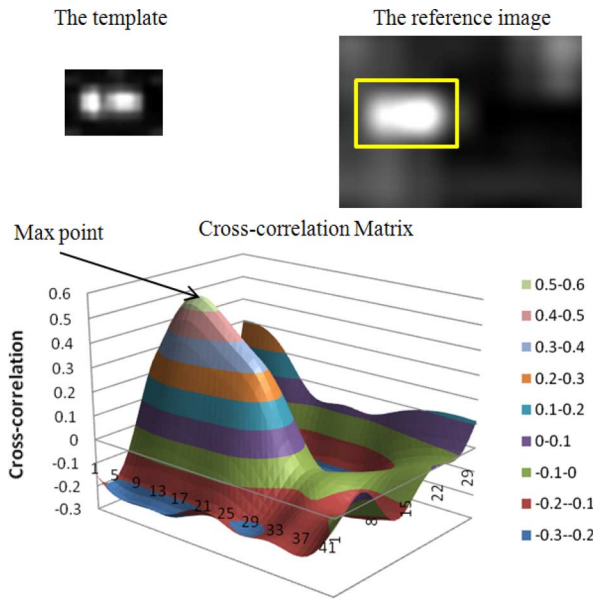

Fig. 4. Example of the cross-correlation matrix obtained by shifting a template over a reference image.

A visual comparison of the results shows that the vehicle templates were accurately matched with the reference extracted from the MS image. However, it is difficult to access the accuracy of this sub-pixel level extraction only from the visual comparison.

Thus, two 0.12 m resolution consecutive digital aerial images taken by UltraCamD camera [24], with both the PAN and MS bands, were employed in a simulation to verify the accuracy of the proposed method. The UltraCamD camera has one PAN band and four (B, G, R and NIR) MS bands, and the wavelengths of the MS bands were similar with those of the QB sensor. The MS digital aerial images were transformed into new 4-band images by PCA, and the first-component images were used. To simulate a QB image, a 13-bit radiometric-resolution aerial image was transformed to an 11-bit image. Since the time lag between two consecutive aerial images is approximately 3 s, they could also be used to determine the speeds of moving vehicles. However, with a time lag of 3 s, the vehicle shift is large. To adjust for this difference, the vehicle templates and reference images were selected manually. A target vehicle was extracted by the object-based method from the two consecutive images.

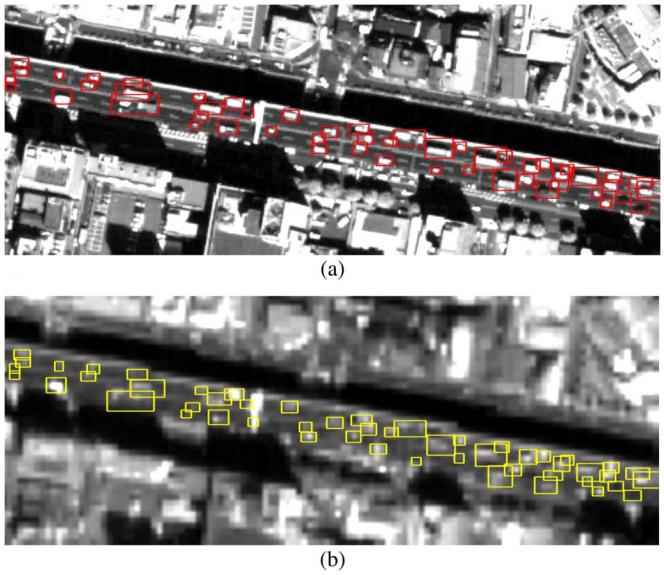

Fig. 5. (a) Vehicle template locations in PAN image and (b) the identified locations in MS image from Study Area II of QuickBird.

Based on the extraction results, a template was selected from the first image that included the target vehicle object and surrounding road, and a reference was selected from the second image, which was bigger than the template. In order to compare with the vehicle extraction from QB images, the pixels of the original PAN image were also resized from 0.12 m to 0.24 m. The reference image extracted from the second image was overlaid by the template from the first image and the cross-correlation matrix was obtained. Since the digital aerial images had a high spatial resolution, the result was considered to be accurate.

Then, the resolution of the PAN image from the first image was converted to 0.6 m/pixel, simulating a PAN image from QB. The resolution of the MS image from the second aerial image was also converted to 2.4 m/pixel, simulating an MS image from QB. The first component of the MS PCA image was used to calculate the cross-correlation matrix with the simulated PAN image. To register the two images at a sub-pixel level, cubic convolution was used to resize the pixels of the two images to 0.24 m. The template and reference images were selected from the simulated PAN and MS images at the same location, as in the original high-resolution images. The cross-correlation matrix was obtained by shifting the simulated PAN image over the MS image.

A comparison of the results with the original data, shown in Fig. 6, the average of the difference along the x axis (the direction of motion) was approximately 2 pixels (0.48 m), and that along the y axis (the transverse direction) was approximately 4 pixels (0.96 m). Since the width of a vehicle is less than 2.4 m, this bigger difference in width is due to a mixed-pixel effect. However, the area correlation method could still extract a vehicle from an MS image with a resolution of 2.4 m at the sub-pixel level.

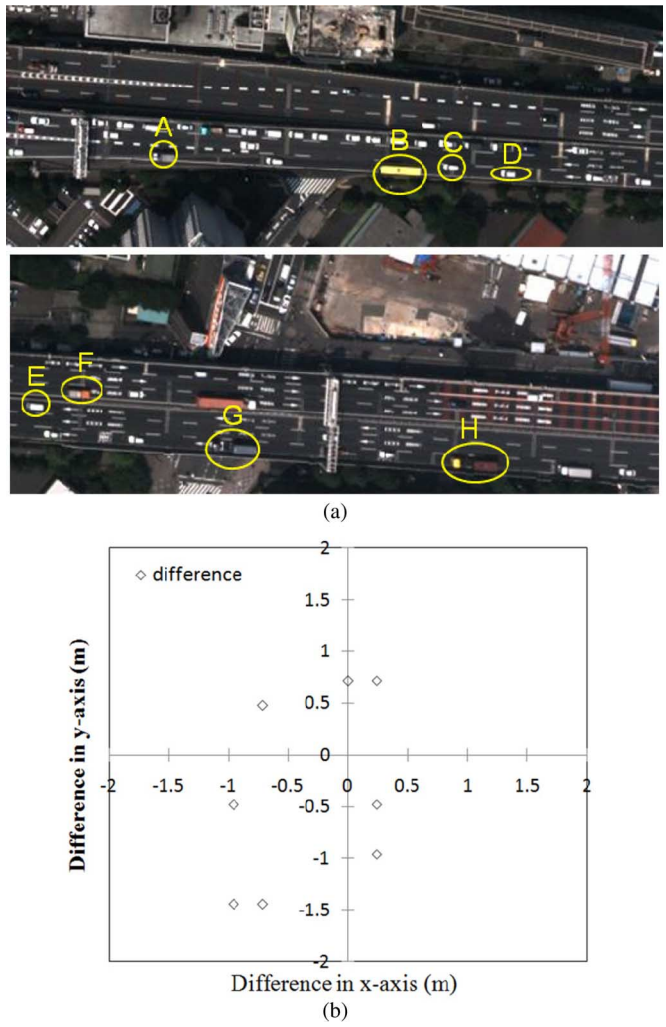

Fig. 6. (a) Eight target vehicles (A-H) in digital aerial image simulation and (b) the difference between the automated vehicle extraction result and the correct location.

VII. Speed Determination From QB Images

The speed of a moving vehicle can be computed by determining the change in the vehicle's location between the PAN and MS images due to the time lag of approximately 0.2 s.

The previous sections showed how moving vehicles were extracted from the three parts of the Tokyo QB PAN and MS images. The movement during the time lag can be calculated from the positions of the vehicle in the two images. Vehicles could not be distinguished clearly in the 2.4 m resolution MS image. Thus, the speed determination results could not be compared with visual inspection. However, as shown in Fig. 7, the results represent realistic speeds. In the upper lane, where vehicles are moving from west to east, the traffic is light enough to run in a high speed. The speeds of vehicles in the lane are around 100 km/h, almost following the speed limit 80 km/h. But in the lower lane, where vehicles are running from east to west, a traffic jam starts at the left edge of this image. Thus, the speeds of vehicles slow down as the vehicles go west. It is also observed that if the space in front of a vehicle is large, the car tends to run

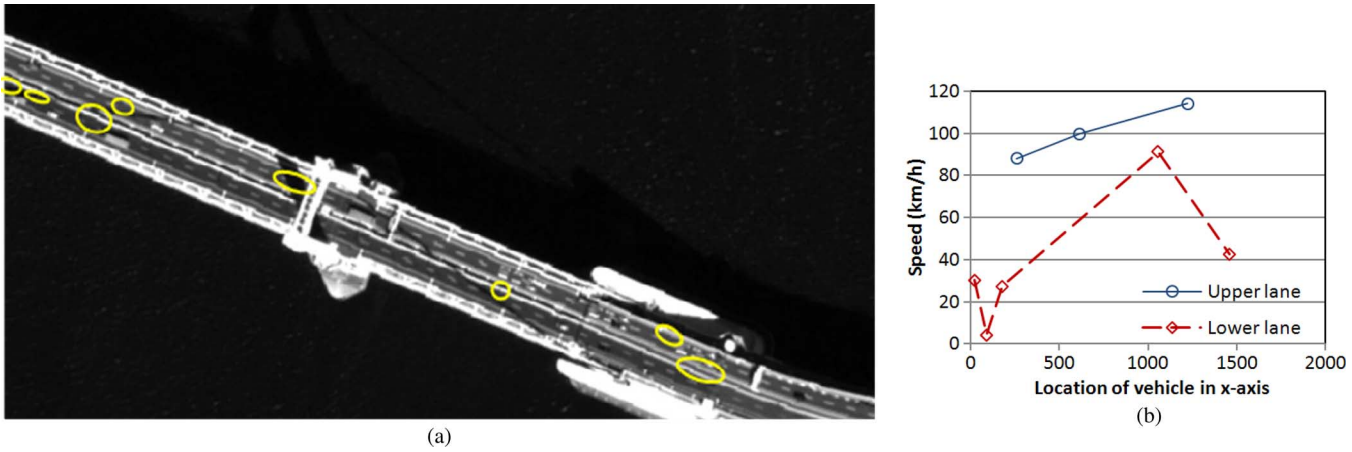

(a) (b)

Fig. 7. (a) Target vehicles in the PAN image and (b) the result of speed detection from Study Area I of QuickBird.

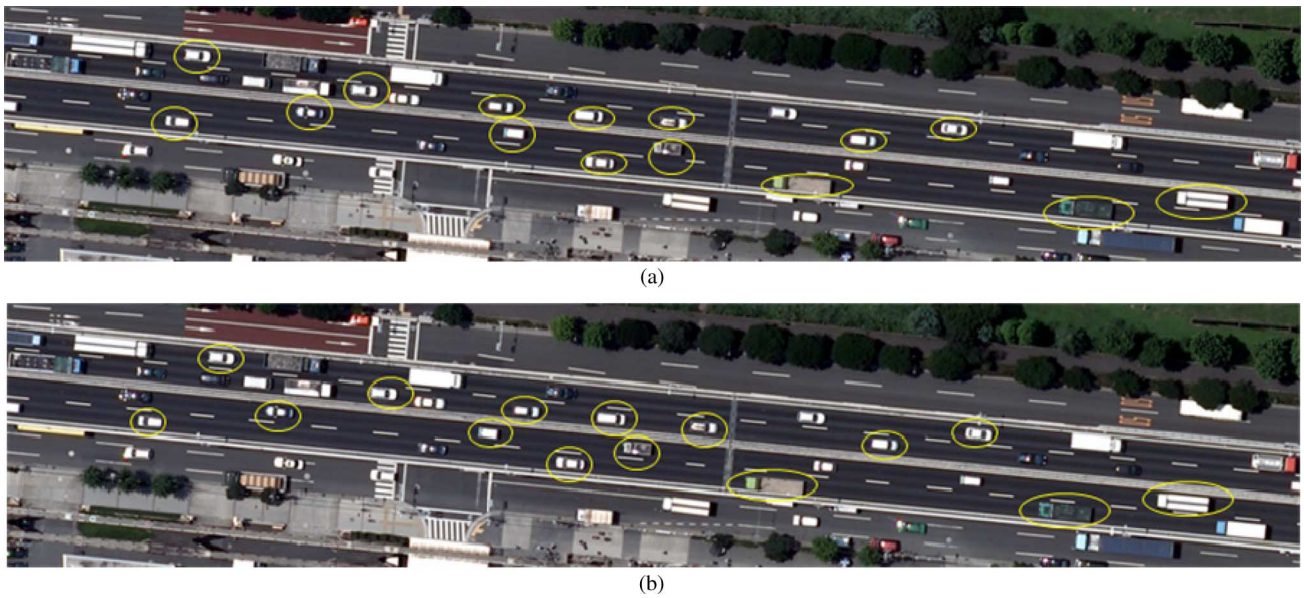

(a) (b)

Fig. 8. (a) Digital aerial image with 0.12 m resolution and (b) simulated aerial image after 0.2 s, produced by moving several vehicles manually.

fast. Thus, the distances between adjacent cars can be an important factor to estimate vehicle speeds.

A simulation was also carried out using the digital aerial images to verify the speed determination accuracy. First, the target vehicles were extracted and moved manually to create a simulated second image (Fig. 8). The movements were recorded as the reference data. Then, the original digital image was transformed to give it a 0.6 m resolution, simulating a PAN image, and the second image was transformed into a 2.4 m resolution image, simulating an MS image. The two simulated QB images are shown in Fig. 9. Vehicle extraction and speed determination were applied to these two simulated images. The speed determination result was then compared with the reference data. The speeds of all of the target vehicles were determined from the simulated images. A comparison with the reference data, as shown in Fig. 10, showed that the standard deviation for the difference in speed between the automated result and the reference was approximately 16 km/h. The speed determination accuracy depends on the vehicle extraction accuracy. Since the vehicle extraction error from the MS image is approximately 0.9 m, the vehicle movement accuracy is in the range of ± 0.9 m. The speed determination accuracy is ± 16 km/h (the speed of a vehicle moving 0.9 m in 0.2 s).

More examples are necessary to verify the vehicle extraction and speed determination accuracies. Since the proposed approach only considers the displacement, the accuracy of the method might be improved by introducing a rotation angle between the template and reference to the area correlation method.

VIII. Conclusion

Methods to extract moving vehicles from QB images and subsequently calculate their speeds have been proposed. First, vehicles were extracted automatically by using an object-based approach from a QB PAN image with a resolution of 0.6 m. Three parts of a QB image of central Tokyo were used to test the effectiveness of the approach, and 94% of the vehicles were successfully extracted. Further, an area correlation method was employed to accurately extract the locations of these vehicles from

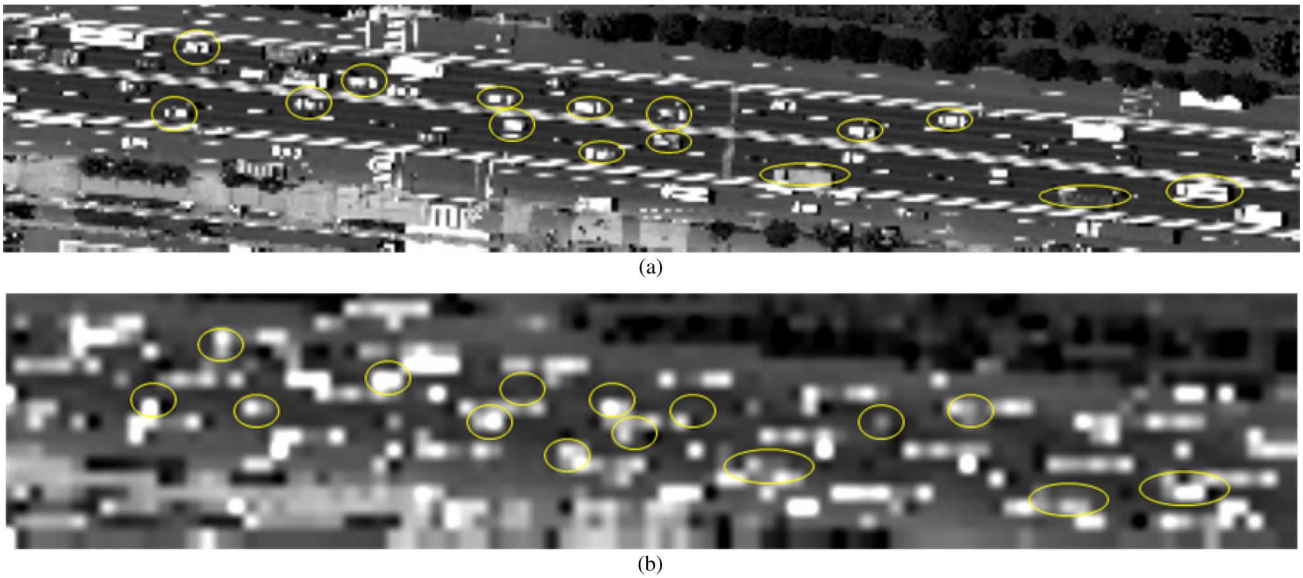

Fig. 9. (a) Simulated PAN image with 0.6 m resolution and (b) simulated MS image with 2.4 m resolution both created from the two aerial images in Fig. 8.

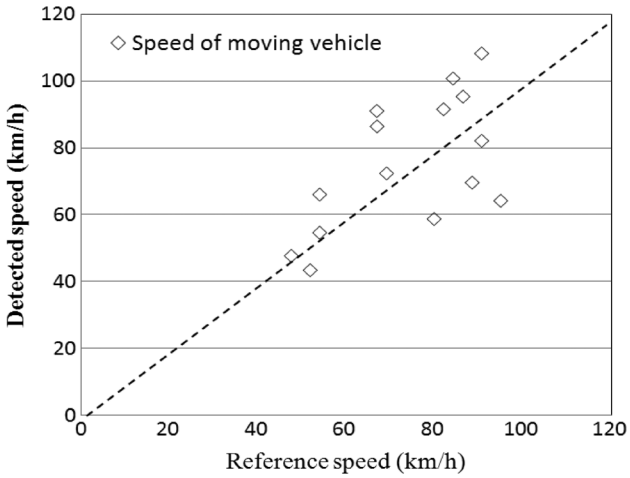

Fig. 10. Comparison of the automatically determined speed and the actual speed.

an MS image with a resolution of 2.4 m at a sub-pixel level. A simulation using digital aerial images revealed that vehicles could be determined with a sub-pixel level accuracy (1/3 pixel for the MS image) for digital images having the spatial resolution of the QB sensors. Since quality differences are seen between the QB image and the simulated one, the accuracy of vehicle extraction from QB images may be less than that expected from the simulation. A further study may be necessary to verify the accuracy of vehicle extraction.

The speed of a moving vehicle could be determined from the difference in the vehicle's positions in a PAN and MS image pair. Due to the limitation of extracting vehicles from a MS image, highly accurate speed determination cannot be expected. From the results of a simulation, it was found that the speed of a moving vehicle can be determined from a QB bundle product to within an error range of ± 16 km/h.

ACKNOWLEDGMENT

The digital aerial images used in this study were provided by the Geographical Survey Institute of Japan.

REFERENCES

[1] M. Dubuisson and A. K. Jain, "Contour extraction of moving objects in complex outdoor scenes," *Int. J. Comput. Vis.*, vol. 14, no. 1, pp. 83–105, 1995.

[2] G. Liu and J. Li, "Moving target detection via airborne HRR phased array radar," *IEEE Trans. Aerosp. Electron. Syst.*, vol. 37, no. 3, pp. 914–924, 2001.

[3] S. Nag and M. Barnes, "A moving target detection filter for an ultra-wideband radar," in *Proc. IEEE Radar Conf. 2003*, May 2003, vol. 5, no. 8, pp. 147–153.

[4] M. Etaya, T. Sakata, H. Shimoda, and Y. Matsumae, "An experiment on detecting moving objects using a single scene of QuickBird data," *J. Remote Sens. Soc. Jpn.*, vol. 24, no. 4, pp. 529–551, 2004.

[5] Z. Xiong and Y. Zhang, "An initial study on vehicle information extraction from single pass of satellite QuickBird imagery," *Photogramm. Eng. Remote Sens.*, vol. 74, no. 11, pp. 1401–1411, 2008.

[6] A. Gerhardinger, D. Ehrlich, and M. Pesaresi, "Vehicles detection from very high resolution satellite imagery," in *CMRT05, IAPRS*, 2005, vol. XXXVI, pp. 83–88, part3/W24.

[7] T. Zhao and R. Nevatia, "Car detection in low resolution aerial image," *Image Vis. Comput.*, vol. 21, no. 8, pp. 693–703, 2003.

[8] X. Jin and C. H. Davis, "Vehicle detection from high-resolution satellite imagery using morphological shared-weight neural networks," *Image Vis. Comput.*, vol. 25, no. 9, pp. 1422–1431, 2007.

[9] J. Leitloff, S. Hinz, and U. Stilla, "Automatic vehicle detection in space images supported by digital map data," in *CMRT05, IAPRS*, 2005, vol. XXXVI, pp. 75–80, part3/W24.

[10] Y. Li, "Vehicle extraction using histogram and genetic algorithm based fuzzy image segmentation from high resolution UAV aerial imagery," in *IAPRS*, 2008, vol. XXXVII, pp. 529–534, part B3b.

[11] G. Sharma, C. J. Merry, P. Goel, and M. McCord, "Vehicle detection in 1-m resolution satellite and airborne imagery," *Int. J. Remote Sens.*, vol. 27, no. 4, pp. 779–797, 2006.

[12] U. Stilla, E. Michaelsen, U. Soergel, S. Hinz, and J. Ender, "Airbone monitoring of vehicle activity in urban areas," in *IAPRS*, 2004, vol. 35, pp. 973–979, Commission III.

[13] M. Kirchhof and U. Stilla, "Detection of moving objects in airborne thermal videos," *ISPRS J. Photogramm. Remote Sens.*, vol. 61, no. 3–4, pp. 187–196, 2006.

[14] J. Leitloff, S. Hinz, and U. Stilla, "Inferring traffic activity from optical satellite images," in *IAPRS*, 2007, vol. 36, no. 3/W49B, pp. 89–93.

[15] M. R. McCord, C. J. Merry, and P. Goel, "Incorporating satellite imagery in traffic monitoring programs," presented at the North American Travel Monitoring Exhibition and Conf., Charlotte, NC, 1998.
[16] Y. Zhang and Z. Xiong, "Moving vehicle detection using a single set of QuickBird imagery—An initial study," *ISPRS*, pp. 397–402, 2006, Commission VII.
[17] M. Pesaresi, K. H. Gutjahr, and E. Pagot, "Estimating the velocity and direction of moving targets using a single optical VHR satellite sensor image," *Int. J. Remote Sens.*, vol. 29, no. 4, pp. 1221–1228, 2008.
[18] R. Nevatia and K. R. Babu, "Linear feature extraction and description," *Comput. Graph. Image Process.*, vol. 13, no. 3, pp. 257–269, 1980.
[19] A. Baumgartner, C. Steger, H. Mayer, W. Eckstein, and H. Ebner, "Automatic road extraction based on multi-scale, grouping, and context," *Photogramm. Eng. Remote Sens.*, vol. 65, no. 7, pp. 777–785, 1999.
[20] A. Katartzis, H. Sahli, V. Pizurica, and J. Cornelis, "A model-based approach to the automatic extraction of linear features from airborne images," *IEEE Trans. Geosci. Remote Sens.*, vol. 39, no. 9, pp. 2073–2079, 2001.
[21] T. T. Vu, M. Matsuoka, and F. Yamazaki, "Dual-scale approach for detection of tsunami-affected areas using optical satellite images," *Int. J. Remote Sens.*, vol. 28, no. 13–14, pp. 2995–3011, 2007.
[22] R. A. Schowengerdt, *Remote Sensing, Models and Methods for Image Processing*, 2nd ed. New York: Academic Press, 2007, ch. 8, pp. 358–365.
[23] L. G. Brown, "A survey of image registration techniques," *ACM Computing Survey*, vol. 24, no. 4, pp. 325–376, 1992.
[24] E. Honkavaara and L. Markelin, "Radiometric performance of digital image data collection—A comparison of ADS40/DMC/UltraCam and EmergeDSS," *Photogrammetrische Woche*, pp. 117–129, 2007.

Wen Liu (S'10) was born in Hangzhou, China, in 1985. She received the B.S. and M.S. degrees in civil engineering from Chiba University, Japan, in 2008 and 2010, respectively. She is currently pursuing the Ph.D. degree at the same university.

Her research interest is urban remote sensing using very high resolution optical sensors and Synthetic Aperture Radar.

Fumio Yamazaki (M'03) was born in Ishikawa, Japan, on May 27, 1953. He received the M.S. degree in civil engineering from the University of Tokyo, Japan, in 1978. After serving as a Visiting Scholar at Columbia University, New York, NY, during 1984–1986, he received the Ph.D. degree in civil engineering from the University of Tokyo in 1987.

He is currently a Professor of Urban Environment Systems, Graduate School of Engineering at Chiba University, Chiba, Japan. He was as a Research Engineer at Shimizu Corporation, Japan, and worked as an Associate Professor at the University of Tokyo and a Professor at Asian Institute of Technology, Thailand. His research interests include stochastic engineering mechanics, earthquake engineering, and more recently, application of GIS and remote sensing technologies to disaster management.

Prof. Yamazaki is a member of Japan Society of Civil Engineers, American Society of Civil Engineers, Earthquake Engineering Research Institute, Seismological Society of America, etc.

Tuong Thuy Vu (M'10) received the M.Sc. and Ph.D. degrees both in geoinformatics from the Asian Institute of Technology, Thailand, in 2000 and 2003, respectively.

He is currently with the Royal Institute of Technology, Stockholm, Sweden. From 2007 to 2008 he was with the GEO Grid group, the National Institute of Advanced Industrial Science and Technology (AIST), Japan. Prior to joining Chiba University (2006–2007) as a postdoctoral researcher, he was a Research Scientist of Earthquake Disaster Mitigation Research Center, Japan, from 2003 to 2006. His current research interests include development of remote sensing image processing algorithms, and applications to disaster management and sustainable development.